ORIGINAL ARTICLE

Quantitative Neuroanatomical Measurement on Photogrammetric Model: Validation Study

Amedeo Piazza[1,2], Jacopo Bellomo[3,4], Sergio Corvino[2,5], Edoardo Agosti[6], Simona Serioli[6], Alice Campeggi[7], Francesco Corrivetti[2], Luca Regli[3,4], Carlo Serra[3,4], Matteo de Notaris[2,8]

■ OBJECTIVE: **To examine and compare the accuracy of measurements obtained from photogrammetric models versus direct measurements taken on dry skulls, with the aim to verify the feasibility of photogrammetry for quantitative analysis in microsurgical neuroanatomy.**

■ METHODS: **Two dry human skulls were used. Each was scanned using the dual camera system of a smartphone The selected photos were separately processed using 2 different softwares to create three-dimensional models. Subsequently, 41 anatomical measurements (both linear and curvilinear) based on common anatomical landmarks were taken both directly on dry skulls and on photogrammetric models and compared. Analyzed factors included measurement error, intrarater and interrater reliability, and intermodality agreement.**

■ RESULTS: **Four photogrammetric models were created. Analysis revealed similar errors when comparing photogrammetric and direct measurements. Measurements from digital models exhibited robust reliability among repeated measures and different observers, supported by very high intraclass correlation coefficient values. Mean measurement difference between Agisoft Metashape software—generated models and direct measurement was 0.01 cm with no systematic bias observed. Conversely, the Metascan app—derived models showed a mean measurement difference of −0.35 cm compared with direct measurement, displaying good agreement for smaller measurements and a systematic proportional bias with increasing measurement size.**

■ CONCLUSIONS: **Two photogrammetric models were validated as quantitative analysis techniques for laboratory neuroanatomical studies, showing acceptable measurement error, high intrarater and interrater reliability, and good to very good agreement compared with direct measurement on dry skulls, replacing expensive and time-consuming methods such as computed tomography scans and neuronavigation systems.**

INTRODUCTION

Microsurgical neuroanatomy plays a pivotal role in the field of neurosurgery.[1] Its application in neurosurgery is instrumental in exploring novel surgical pathways that demand a nuanced understanding of complex techniques and approaches.[2] Precise measurements on anatomical specimens allow for enhanced accuracy and efficacy of surgical planning and execution. Historically, neuroanatomical

Key words
- Neuroanatomy
- Photogrammetry
- Quantitative analysis
- Skull base
- Surgical corridor

Abbreviations and Acronyms
3D: Three-dimensional
CT: Computed tomography
ICC: Interclass correlation coefficient
LoA: Limits of agreement

From the [1]Department of Neurosurgery, Sapienza University of Rome, Rome, Italy; [2]Laboratory of Neuroscience, European Biomedical Research Institute of Salerno Foundation, Salerno, Italy; [3]Department of Neurosurgery, University Hospital Zurich, Zurich, Switzerland; [4]Clinical Neuroscience Center, Neuroscience Center, University of Zurich, Zurich, Switzerland; [5]Reproductive and Odontostomatological Sciences, Division of Neurosurgery, Department of Neuroscience, University of Naples Federico II, Naples, Italy; [6]Division of Neurosurgery, Department of Medical and Surgical Specialties, Radiological Sciences and Public Health, University of Brescia, Brescia, Italy; [7]Surgical and Medical Sciences and Translational Medicine, Sapienza University of Rome, Rome, Italy; and [8]Unit of Neurosurgery, University Hospital San Giovanni di Dio e Ruggi d'Aragona, University of Salerno, Salerno, Italy

Amedeo Piazza and Jacopo Bellomo contributed equally as co—first authors.

To whom correspondence should be addressed: Sergio Corvino, M.D., Ph.D. [E-mail: sercorvino@gmail.com]

Citation: World Neurosurg. (2025) 194:123574. https://doi.org/10.1016/j.wneu.2024.123574

Journal homepage: www.journals.elsevier.com/world-neurosurgery

Available online: www.sciencedirect.com

measurements were laboriously performed manually, employing tools such as compasses, rulers, and caliper. The advent of computed tomography (CT) marked a significant leap forward, supplanting manual approaches and ushering in the ability to conduct volumetric measurements.[3,4] Despite remarkable progress and development of significant technological support, further advancement in neuroanatomical research on a broader scale currently encounters considerable obstacles—mainly, CT machines are restricted to only a small number of laboratories, and availability of neuronavigation systems is still limited.

In response to these challenges, photogrammetry has emerged as a cutting-edge technique.[5,6] Initially employed for aerial surveys[7] and archaeological purposes,[8] photogrammetry is progressively finding applications in neuroanatomy.[9-12] This method enables the creation of three-dimensional (3D) models from two-dimensional photographs, using both readily available devices, such as smartphones, and specialized software programs.[13,14]

This study examined and compared the precision of measurements obtained from photogrammetric models against direct measurements taken on dry skulls. This comparative analysis aimed to evaluate the reliability and accuracy of photogrammetry as a measurement tool in neuroanatomy. Photogrammetry has the potential to be a breakthrough alternative, with the advantage of being widely applicable and more accessible than traditional techniques, particularly in settings where CT resources are limited. As technology continues to evolve, integrating innovative methods such as photogrammetry may pave the way for enhanced neuroanatomical research methodologies and contribute to advancements in neurosurgical practices.

MATERIALS AND METHODS

Study Design

This study employed a cross-sectional design to validate a novel measurement method using photogrammetry 3D models against direct measurements taken from anatomical specimens. The goal was to assess the accuracy, reliability, and agreement of measurements obtained through the photogrammetric approach compared with traditional direct measurements.

Head Specimens

Two dry human skulls were used for this study. The dry skull was obtained as previously described.[15] The skulls were marked with a black marker. The marks were used as coordinates to permit linear and curvilinear measurements.

Ethics

In accordance with Italian law and the policies of our institution, we hereby state that the use of specimens for academic research purposes within the scope of this study does not require formal approval from an ethics committee. Our practices comply with all relevant national regulations governing the ethical use of such specimens in a research setting.

Photogrammetry Software

In this study, 2 different software programs were used: Agisoft Metashape (Agisoft LLC, St. Petersburg, Russia) and Metascan (Abound Labs Inc., New York, New York, USA). Agisoft Metashape and Metascan are designed for different purposes and cater to distinct audiences, even though both focus on creating 3D models. Metashape is a professional photogrammetry software widely used for creating highly detailed 3D reconstructions, whereas Metascan is typically associated with quick 3D scanning designed for mobile devices. It is more suited to smaller-scale projects, rapid prototyping, and consumer-friendly applications.

The workflows also differ significantly. Metashape offers a customizable and highly detailed process, making it ideal for handling large datasets. However, it requires significant computational resources and some expertise. In contrast, Metascan is designed for ease of use, with a streamlined process that requires minimal setup and is ideal for quick scans.

In terms of input, Metashape relies on high-resolution images from professional cameras or drones, requiring significant overlap between images for accuracy. Metascan, by comparison, often works with lower-resolution inputs, including photos or videos captured with smartphones or tablets. The output quality reflects this difference: Metashape delivers professional-grade models and detailed geospatial data, whereas Metascan produces simpler models. Hardware requirements also differ, with Metashape needing powerful computers for optimal performance, whereas Metascan is optimized for smartphones.

Metashape is a paid software intended for professionals and institutions, offering licenses for its standard and professional versions. Metascan is generally more affordable.

Photogrammetry Model

Each dry skull was scanned using the dual camera system of an iPhone 11 Pro (Apple Inc., Cupertino, California, USA). A total of 180 photos were taken for each skull, and any photos out of focus or out of the field were discharged. The photos selected for each skull were separately processed using either Metascan App or Agisoft Metashape professional edition 2.1 to create 3D models from the 2 dry skulls. Metascan app automatically scales the model, whereas Agisoft Metashape requires manual scaling according to a known measure used as a reference. Outer coronal diameter of the dry skulls was used as a reference distance to scale Agisoft Metashape models. To assess the quality of the photogrammetric models, the density of the mesh was evaluated based on the following parameters: number of vertices, edges, faces, and face corners.

Anatomical Landmarks and Measurements

A total of 41 different anatomical measures were defined based on common anatomical landmarks. These included 23 linear measures (inner sagittal diameter, inner coronal diameter, interoptic foramen distance, interclinoidal distance, sagittal clivus height, sagittal foramen magnum diameter, coronal foramen magnum diameter, longest and shortest diameter of the right and left foramen ovale, right and left arcuate eminence, right and left horizontal orbital diameter, right and left vertical orbital diameter, right and left superior orbital fissure length, right and left inferior orbital fissure length, horizontal nasal cavity diameter, vertical nasal cavity diameter) and 18 curvilinear measures (right and left frontoparietal curve, right and left parieto-occipital curve, right and left anterior foramen magnum curve, right and left posterior foramen magnum curve, right and left transverse sinus groove, right and left sigmoidal sinus groove, right and left great wing of sphenoid bone, right and left lateral supraorbital margin, right and left lateral infraorbital margin).

Measurement Techniques

Measurements were acquired both directly and via the 2 photogrammetric models (Metascan model and Agisoft Metashape model). Each measurement was performed independently by 2 different observers (A.P. and J.B.) and repeated twice in separate sessions on different days. This resulted in 12 measurement sessions for each observer: 4 direct measurement sessions on 2 dry skulls, 4 with Metascan model, and 4 with Agisoft Metashape model. Each observer was blinded to the measurements acquired during their other sessions and to the measurements acquired from the other observer. For the direct measurement technique, linear and curvilinear measurements were first acquired through direct measurement on both dry skulls using a rigid and flexible ruler, respectively, with a measurement uncertainty of 0.1 cm.

Measurement Technique on Photogrammetric Models

3D models were imported into Blender.[16] Subsequently, linear measurements were taken using the tool "ruler" and the function "snap to face project" (Figure 1). Curvilinear measurements were taken using the tool "curve distance" with the function "snap to face project" (Figure 1).

Statistical Analysis

Statistical analysis was conducted using the statistical program RStudio version 02.07.2022 (Posit Software, PBC formerly R Studio, Boston, Massachusetts, USA).

Measurement Error Analysis. A comprehensive measurement error analysis was conducted to evaluate the precision of direct measurement and measurements obtained through photogrammetry. For both observers, the within-measurement standard deviation was calculated to quantify the variability within each set of measurements. The within-measurement variance was derived using 1-way analysis of variance, enabling the computation of the standard deviation, providing a robust assessment of measurement error.

Intrarater and Interrater Reliability. Intrarater and interrater reliability was assessed for both direct measurements and photogrammetry models to gauge the consistency of the repeated measurements of the same observer and between different observers. The intraclass correlation coefficient (ICC) was employed as a quantitative measure of intrarater and interobserver consistency. ICC values vary from 0 to 1, with higher values indicating better agreement.

Intermodality Agreement Analysis. The Bland-Altman method[17] was used to examine the agreement between measurements obtained through photogrammetric models and direct measurements. Bland-Altman plots were generated to visually represent the mean difference and limits of agreement (LoA). These plots offer a comprehensive view of the systematic bias and random error between the 2 measurement methods, providing valuable insights into their agreement.

RESULTS

Photogrammetric Models

Four photogrammetric models were generated. Two 3D models were generated from dry skull 1, and 2 were generated from dry skull 2. Mesh analysis of the model generated with Metascan showed 47,808 vertices, 139,233 edges, 92,207 faces, and 276,621 face corners for dry skull 1 and 33,638 vertices, 10,000 edges,

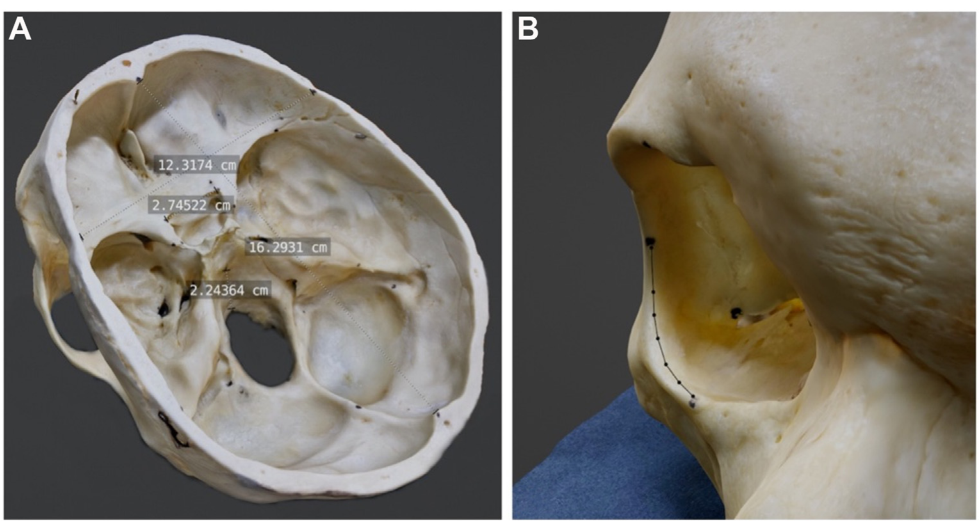

Figure 1. Example of measurement on Blender. (**A**) Linear measurements. (**B**) Curvilinear measurement.

66,350 faces, and 199,050 face corners for dry skull 2. Mesh analysis of the model generated with Agisoft Metashape showed 192,125 vertices, 573,586 edges, 381,446 faces, and 1,144,338 face corners for dry skull 1 and 139,896 vertices, 417,696 edge, 277,889 faces, and 833,667 face corners for dry skull 2.

Measurement Error

The precision of direct measurements and measurements derived from Metascan app–generated and Agisoft Metashape software–generated models on the 2 dry skulls were evaluated for each observer. Within-measurement variance and standard deviation were computed and are presented in Table 1. The analysis showed that the magnitude of errors influencing measurements obtained from photogrammetry models closely mirrored those encountered in direct measurements. Notably, these errors did not exhibit a correlation with the size of the measurements. The precision of direct measurements taken from dry skulls was approximately 1 mm for both observers. In the case of the Metascan model, the measurement error was also approximately 1 mm, whereas for the Agisoft Metashape model, the observed errors were <1 mm. In general, curvilinear measurements exhibited lower precision compared with linear ones.

Intrarater and Interrater Reliability

Intrarater reliability for repeated measurements was assessed for the different techniques. We found very high intrarater consistency for photogrammetric models comparable to what was observed from the direct measurement. The agreement between observers was investigated through interrater reliability. Measurements extracted from digital models showed a high level of agreement between the 2 independent observers. The robust intrarater and interrater reliability is substantiated by ICC values approaching unity, as detailed in Tables 2 and 3, respectively.

Measurement Agreement Between the 2 Methods

The agreement between measurements from photogrammetric models and direct measurement was explored using Bland-Altman plots. A very good agreement was observed for the Agisoft Metashape software–generated model, with a mean difference of 0.01 cm (lower LoA −0.21, upper LoA 0.23) and no discernible systematic proportional bias (Figure 2B). Conversely, the agreement for Metascan app–derived models remained good for smaller measurements, but exhibited a systematic proportional bias with increasing measurement size (Figure 2A). In fact, there was poor agreement for measurements >5 cm with differences between the 2 techniques >1 cm. Overall, we determined a mean difference of −0.35 cm (lower LoA −1.10, upper LoA 0.39). Comparable results were obtained when analyzing linear and curvilinear measurements separately, as illustrated in Supplementary Figures 1 and 2.

DISCUSSION

Over the years, cadaveric anatomical studies based on microsurgical dissections have led to the progressive discovery of key anatomical surgical landmarks and new operative corridors and to the development of increasingly minimally invasive approaches. Lately, many technological tools have been proposed as alternative or complementary methods to the cadaveric dissections for several purposes, such as anatomical education, surgical training, and morphometric qualitative and/or qualitative analysis. These innovative tools include 3D printing,[18-21] virtual augmented reality,[22] surgical simulation,[23] and, more recently, photogrammetry,[11,12,24,25] each carrying unique benefits. In particular, photogrammetry was used for educational,[5,26-28] neuroanatomy,[25,27,29-31] and clinical application.[9,32,33] In this setting, the assessment of measurements, including distance between ≥2 points defining key anatomical structures, volumes of entry and/or target areas, exposure and/or working areas, as well as of surgical corridor, first is very

Table 1. Measurement Errors

	All Measurements (cm)			Only Linear Measurements (cm)			Only Curvilinear Measurements (cm)		
	σ^2	σ	95% CI	σ^2	σ	95% CI	σ^2	σ	95% CI
Real skull									
Observer 1	0.012	0.110	0.086–0.135	0.007	0.081	0.057–0.105	0.020	0.140	0.093–0.187
Observer 2	0.007	0.086	0.067–0.104	0.003	0.059	0.041–0.076	0.012	0.110	0.073–0.148
Metascan model									
Observer 1	0.012	0.111	0.087–0.135	0.002	0.039	0.027–0.051	0.026	0.162	0.107–0.216
Observer 2	0.010	0.082	0.064–0.100	0.001	0.029	0.020–0.037	0.014	0.120	0.079–0.160
Agisoft Metashape model									
Observer 1	0.003	0.046	0.036–0.056	0.001	0.038	0.026–0.049	0.003	0.054	0.036–0.072
Observer 2	0.006	0.076	0.059–0.093	0.005	0.073	0.052–0.095	0.006	0.079	0.052–0.106

For each technique, measurement error is provided through within-measurement variance and SD with 95% CI.
CI, confidence interval.

Table 2. Intrarater Reliability

	ICC
Real skull	
All measurements (cm)	0.999
Linear measurements (cm)	0.999
Curvilinear measurements (cm)	0.998
Metascan model	
All measurements (cm)	0.999
Linear measurements (cm)	0.999
Curvilinear measurements (cm)	0.998
Agisoft Metashape model	
All measurements (cm)	0.999
Linear measurements (cm)	0.999
Curvilinear measurements (cm)	0.999

For each technique, within-observer reliability for repeated measurements is provided through ICC assessment.
ICC, intraclass correlation coefficient.

important for learning anatomy but especially for surgical implications. Until now, CT scan of the head specimen, before and after dissections, using a neuronavigation system, represents the main strategy for these purposes. Nevertheless, this method requires the availability of a neuronavigation system, a CT scanner, and a radiologist, not always available in laboratories, and ultimately is very expensive. To overcome all these limits, we have developed an inexpensive and easily reproducible method, based on photogrammetric technique, which allows calculation, with high degree of precision, of linear and volumetric measurements on microsurgical dissected cadaveric specimens.

Table 3. Interrater Reliability

	ICC
Real skull	
All measurements (cm)	0.999
Linear measurements (cm)	0.999
Curvilinear measurements (cm)	0.999
Metascan model	
All measurements (cm)	0.998
Linear measurements (cm)	0.998
Curvilinear measurements (cm)	0.997
Agisoft Metashape model	
All measurements (cm)	0.999
Linear measurements (cm)	0.999
Curvilinear measurements (cm)	0.999

For each technique, between-observer reliability for each single measurement is provided through ICC assessment.
ICC, intraclass correlation coefficient.

Evaluating the precision of measurements obtained from photogrammetric models is needed to assess reliability and accuracy of photogrammetry as a novel measurement tool in neuroanatomy. The level of details and precision of photogrammetric models is associated with specific characteristics. For instance, the density of meshes is directly proportional to model accuracy. Mesh density refers to the number of points or triangles that constitute the 3D surface generated through photogrammetry. In simple terms, higher mesh density translates to more detailed and accurate representation of the subject in the 3D model.

When applying photogrammetry to generate a 3D model from two-dimensional images, software algorithms identify corresponding points in different images. These points are then used to create a network of triangles approximating the subject's surface. Mesh density is determined by the number of such triangles or points, typically expressed in units of measurement (vertex, edge, face, face corner).

A denser mesh allows for a more precise representation of surfaces and features of the subject, capturing the finest details. However, higher density may result in increased computational resources and storage space usage. Therefore, the choice of mesh density depends on the specific requirements of the application.

In this study, it was confirmed that a higher mesh density was associated with higher precision and reliability in measurements. Nevertheless, even for smaller measurements, e.g., <5 cm, the smartphone app demonstrated the capability to obtain accurate results. In addition, the 2 software programs assessed in this study work differently. Metascan scales the model automatically, whereas Metashape needs to have a known distance to scale the model. That, together with the complexity of the mesh, could be an additional reason why a better agreement was found in the measurement taken in the Metashape models.

When considering the 2 aforementioned photogrammetric models, the analysis revealed similar errors in measurements compared with direct measurement. Measurements from digital models exhibited robust reliability between repeated measures and observers, supported by very high ICC values. Furthermore, Bland-Altman analysis highlighted a remarkable agreement between Agisoft Metashape software—generated models and direct measurement, with no observed systematic proportional bias. Conversely, the Metascan app—derived models displayed good agreement for smaller measurements but demonstrated a systematic proportional bias with increasing measurement size. This issue may be due to a lower-density mesh structure generated by Metascan. We recommend using Metascan only for two-dimensional measurements <5 cm. Nevertheless, this work underlines the validity of photogrammetric models as a measurement technique for neuroanatomical studies. Validating two-dimensional measurements in space inherently validates volumetric measurements as these distances are derived from points with 3D coordinates.

Photogrammetric measurements come with both advantages and disadvantages when compared with CT. The former stand out for their significantly lower cost, which constitutes a notable benefit especially in context of limited financial resources, and for the

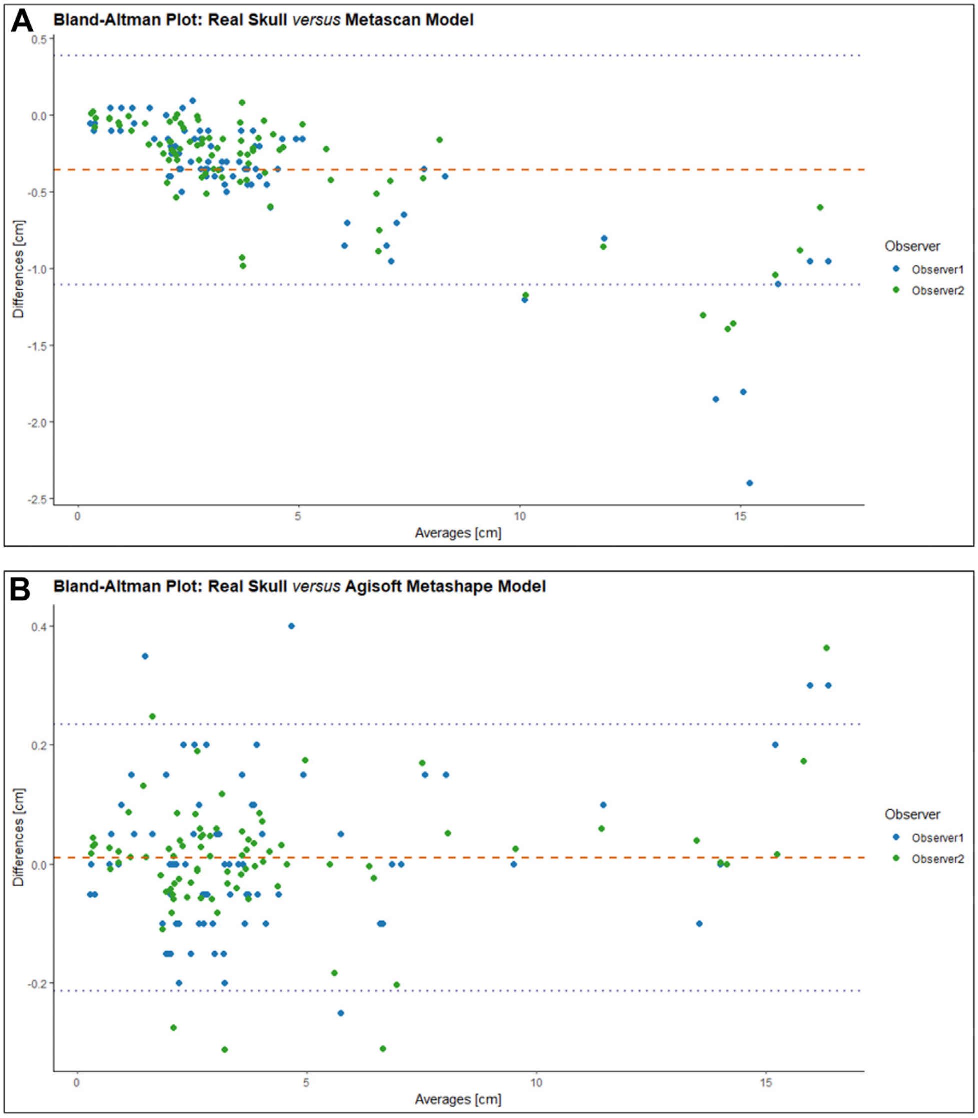

Figure 2. Bland-Altman plots for all measurements. (**A**) Illustration of the agreement of measurements taken with Metascan model compared with direct measurements. A mean difference of −0.35 cm was found with lower limits of agreement (LoA) of −1.10 and upper LoA of 0.39. Notably, a systematic proportional bias was observed for measurements >5 cm. (**B**) Illustration of the agreement of measurements taken with Agisoft Metashape model compared with direct measurements. A mean difference of 0.01 cm was found with lower LoA of −0.21 and upper LoA of 0.23.

possibility to acquire measurements over time. The latter feature represents an important advantage compared with the method of CT scans and neuronavigation: indeed, a 3D reconstructed photogrammetric model not only allows collection of the measurement data, but also acquisition of new measurements of different areas included in dissections from the reconstructed and saved model, at any time and for multiple studies, obviating the problem of the head specimen storage and preservation/decomposition.

Contrastingly, a possible limitation of photogrammetry may lie in the fact that it allows measurements only of areas that have been exposed and reconstructed, which poses problems especially when assessing structures that are not visible superficially. Moreover, as of today, the possibility of conducting measurements on 3D models generated from deep surgical fields, such as the endoscopic endonasal approach, through photogrammetry has not yet been demonstrated.

The potential to perform direct measurements on 3D models could revolutionize the field of neuroanatomy, suggesting a future where volumetric measurements may not require a CT scan or neuronavigation system. On the other hand, the cost of neuronavigation and CT scans, which can exceed $200,000, could potentially be reduced by using a photogrammetric setup. In professional settings, such a setup costs <$6000, and for a smartphone-based system, the cost, including the smartphone, is <$1000. This prospect holds significant promise for laboratories with limited financial resources.

Future studies should aim to assess the agreement between direct measurements and measurements obtained from photogrammetric models generated using endoscopic images. Additionally, studies should explore the feasibility of evaluating maneuverability and volumetric corridors within the generated models. This approach will enhance the ability to compare surgical techniques, ultimately leading to improved surgical approach selection and outcomes.

LIMITATIONS

To the best of our knowledge, this study represents the first validation of photogrammetric models as measurement techniques in the field of neuroanatomy. This comprehensive study was designed to investigate 2 different digital models keeping direct measurements as reference standard and to assess measurement error, intrarater and interrater reliability, and measurement agreement. However, some limitations must be mentioned. Although we investigated 41 measures on 2 different dry skulls, the study may be limited by too little heterogeneity of the measurement sample, which might not adequately represent the variability of a broader population of anatomical specimen. Another important limitation is determined by the choice of the reference standard, i.e., direct measurement using a ruler with measurement uncertainty of 1 mm. On one hand, this represents a widely accepted measurement technique, but on the other, the validation of digital models is limited by its accuracy and reliability.

CONCLUSIONS

In this study, 2 photogrammetric models were validated as measurement techniques for neuroanatomical studies, showing acceptable measurement error, high intrarater and interrater reliability, and good to very good agreement compared with direct measurement on dry skulls. However, a significant difference in the performance of the 2 different models was noted, with the more complex Agisoft Metashape model performing better than the model generated with the Metascan app.

CRediT AUTHORSHIP CONTRIBUTION STATEMENT

Amedeo Piazza: Conceptualization, Data curation, Formal analysis, Investigation, Methodology, Validation, Writing – original draft. **Jacopo Bellomo:** Conceptualization, Data curation, Formal analysis, Investigation, Methodology, Software, Writing – original draft. **Sergio Corvino:** Data curation. **Edoardo Agosti:** Data curation. **Simona Serioli:** Data curation, Formal analysis. **Alice Campeggi:** Data curation, Formal analysis, Methodology. **Francesco Corrivetti:** Data curation. **Luca Regli:** Supervision, Validation. **Carlo Serra:** Supervision, Validation. **Matteo de Notaris:** Supervision, Validation.

REFERENCES

1. Yaşargil MG. A legacy of microneurosurgery: memoirs, lessons, and axioms. *Neurosurgery*. 1999; 45:1025-1092.

2. Kobayashi S, Matsushima T, Sakai T, Matsushima K, Bertalanffy H, Rutka JT. Evolution of microneurosurgical anatomy with special reference to the history of anatomy, surgical anatomy, and microsurgery: historical overview. *Neurosurg Rev*. 2022;45:253-261.

3. de Notaris M, Palma K, Serra L, et al. A three-dimensional computer-based perspective of the skull base. *World Neurosurg*. 2014;82(6 Suppl): S41-S48.

4. Noiphithak R, Yanez-Siller JC, Revuelta Barbero JM, Otto BA, Carrau RL, Prevedello DM. Quantitative analysis of the surgical exposure and surgical freedom between transcranial and transorbital endoscopic anterior petrosectomies to the posterior fossa. *J Neurosurg*. 2018;131:569-577.

5. Spiriev T, Mitev A, Stoykov V, Dimitrov N, Maslarski I, Nakov V. Three-dimensional immersive photorealistic layered dissection of superficial and deep back muscles: anatomical study. *Cureus*. 2022;14:e26727.

6. Xu Y, Vigo V, Klein J, et al. Pursuing perfect 2D and 3D photography in neuroanatomy: a new paradigm for staying up to date with digital technology. *J Neurosurg*. 2022;138:1766-1772.

7. Leberl F, Meixner P, Wendel A, Irschara A. Automated photogrammetry for three-dimensional models of urban spaces. *Opt Eng*. 2012;51:021117.

8. Sužiedelytė-Visockienė J, Bagdžiūnaitė R, Malys N, Maliene V. Close-range photogrammetry enables documentation of environment-induced deformation of architectural heritage. *Environ Engineering Manag J*. 2015;14:1371-1381.

9. Abdel-Alim T, Iping R, Wolvius EB, et al. Three-dimensional stereophotogrammetry in the evaluation of craniosynostosis: current and potential use cases. *J Craniofac Surg*. 2021;32:956-963.

10. Chae R, Sharon JD, Kournoutas I, et al. Replicating skull base anatomy with 3D technologies: a comparative study using 3D-scanned and 3D-printed models of the temporal bone. *Otol Neurotol*. 2020;41:e392-e403.

11. Gonzalez-Romo NI, Hanalioglu S, Mignucci-Jiménez G, Abramov I, Xu Y, Preul MC. Anatomic depth estimation and 3-dimensional reconstruction of microsurgical anatomy using monoscopic high-definition photogrammetry and machine learning. *Oper Neurosurg (Hagerstown)*. 2023;24: 432-444.

12. Petriceks AH, Peterson AS, Angeles M, Brown WP, Srivastava S. Photogrammetry of human specimens: an innovation in anatomy education. *J Med Educ Curric Dev*. 2018;5:2382120518799356.

13. Titmus M, Whittaker G, Radunski M, et al. A workflow for the creation of photorealistic 3D cadaveric models using photogrammetry. *J Anat*. 2023;243:319-333.

14. de Oliveira ASB, Leonel L, LaHood ER, et al. Foundations and guidelines for high-quality three-dimensional models using photogrammetry: a technical note on the future of neuroanatomy education. *Anat Sci Educ*. 2023;16:870-883.

15. Ator GA, Andrews JC, Maxwell DS. Preparation of the human skull for skull base anatomic study. *Skull Base Surg*. 1993;3:1-6.

16. Community, B. O. Blender - a 3D modelling and rendering package. Stichting Blender Foundation, Amsterdam. 2018. Available at: http://www.blender.org. Accessed January 2, 2024.

17. Bland JM, Altman DG. Statistical methods for assessing agreement between two methods of clinical measurement. *Lancet*. 1986;1:307-310.

18. Piazza A, Petrella G, Corvino S, et al. 3-Dimensionally printed affordable nose model: a reliable start in endoscopic training for young neurosurgeons. *World Neurosurg*. 2023;180:17-21.

19. McGuire LS, Fuentes A, Alaraj A. Three-dimensional modeling in training, simulation, and surgical planning in open vascular and endovascular neurosurgery: a systematic review of the Literature. *World Neurosurg*. 2021;154:53-63.

20. Blohm JE, Salinas PA, Avila MJ, Barber SR, Weinand ME, Dumont TM. Three-dimensional printing in neurosurgery residency training: a systematic review of the literature. *World Neurosurg*. 2022;161:111-122.

21. Piazza A, Corvino S, Colosso GQ, et al. 3-Dimensional printed model of the temporal bone for neurosurgical training. *Oper Neurosurg (Hagerstown)*. 2024. https://doi.org/10.1227/ons.0000000000001213.

22. Petrone S, Cofano F, Nicolosi F, et al. Virtual-augmented reality and life-like neurosurgical simulator for training: first evaluation of a hands-on experience for residents. *Front Surg*. 2022;9:862948.

23. Davids J, Manivannan S, Darzi A, Giannarou S, Ashrafian H, Marcus HJ. Simulation for skills training in neurosurgery: a systematic review, meta-analysis, and analysis of progressive scholarly acceptance. *Neurosurg Rev*. 2021;44:1853-1867.

24. Aydin SO, Barut O, Yilmaz MO, et al. Use of 3-dimensional modeling and augmented/virtual reality applications in microsurgical neuroanatomy training. *Oper Neurosurg (Hagerstown)*. 2023;24:318-323.

25. Corvino S, Piazza A, Spiriev T, et al. The Sellar region as seen from transcranial and endonasal Perspectives: exploring Bony landmarks through new surface photorealistic 3D models reconstruction for neurosurgical anatomy training. *World Neurosurg*. 2024;185:e367-e375.

26. Piazza A, Alexander AY, Peris-Celda M, Lanzino G. How I do it: surgical ligation of posteromedial tentorial dural arteriovenous fistulas. *Acta Neurochir*. 2024;166:382.

27. Gurses ME, Gungor A, Hanalioglu S, et al. Qlone®: a simple method to create 360-degree photogrammetry-based 3-dimensional model of cadaveric specimens. *Oper Neurosurg (Hagerstown)*. 2021;21:E488-E493.

28. Krogager ME, Fugleholm K, Mathiesen TI, Spiriev T. Simplified easy-accessible smartphone-based photogrammetry for 3-dimensional anatomy presentation exemplified with a photorealistic cadaver-based model of the intracranial and extracranial course of the facial nerve. *Oper Neurosurg (Hagerstown)*. 2023;25:e71-e77.

29. Piazza A, Corvino S, Ballesteros D, et al. Neuroanatomical photogrammetric models using smartphones: a comparison of apps. *Acta Neurochir*. 2024;166:378.

30. Piazza A, Spiriev T, Corvino S, et al. The course of the trochlear nerve presented with 3-D photorealistic anatomical model. *World Neurosurg*. 2024;186:e156-e160.

31. Corvino S, Kassam A, Piazza A, et al. Navigating the Intersection between the orbit and the skull base: the "mirror" McCarty keyhole during transorbital approach: an anatomic study with surgical Implications. *Oper Neurosurg (Hagerstown)*. 2024. https://doi.org/10.1227/ons.0000000000001274.

32. Krawczky B, Pacheco AG, Mainenti MR. A systematic review of the angular values obtained by computerized photogrammetry in sagittal plane: a proposal for reference values. *J Manip Physiol Ther*. 2014;37:269-275.

33. Pivotto LR, Navarro I, Candotti CT. Radiography and photogrammetry-based methods of assessing cervical spine posture in the sagittal plane: a systematic review with meta-analysis. *Gait Posture*. 2021;84:357-367.

Conflict of interest statement: The authors declare that the article content was composed in the absence of any commercial or financial relationships that could be construed as a potential conflict of interest.

Received 20 November 2024; accepted 9 December 2024

Citation: World Neurosurg. (2025) 194:123574.
https://doi.org/10.1016/j.wneu.2024.123574

Journal homepage: ***www.journals.elsevier.com/world-neurosurgery***

Available online: ***www.sciencedirect.com***

SUPPLEMENTARY DATA

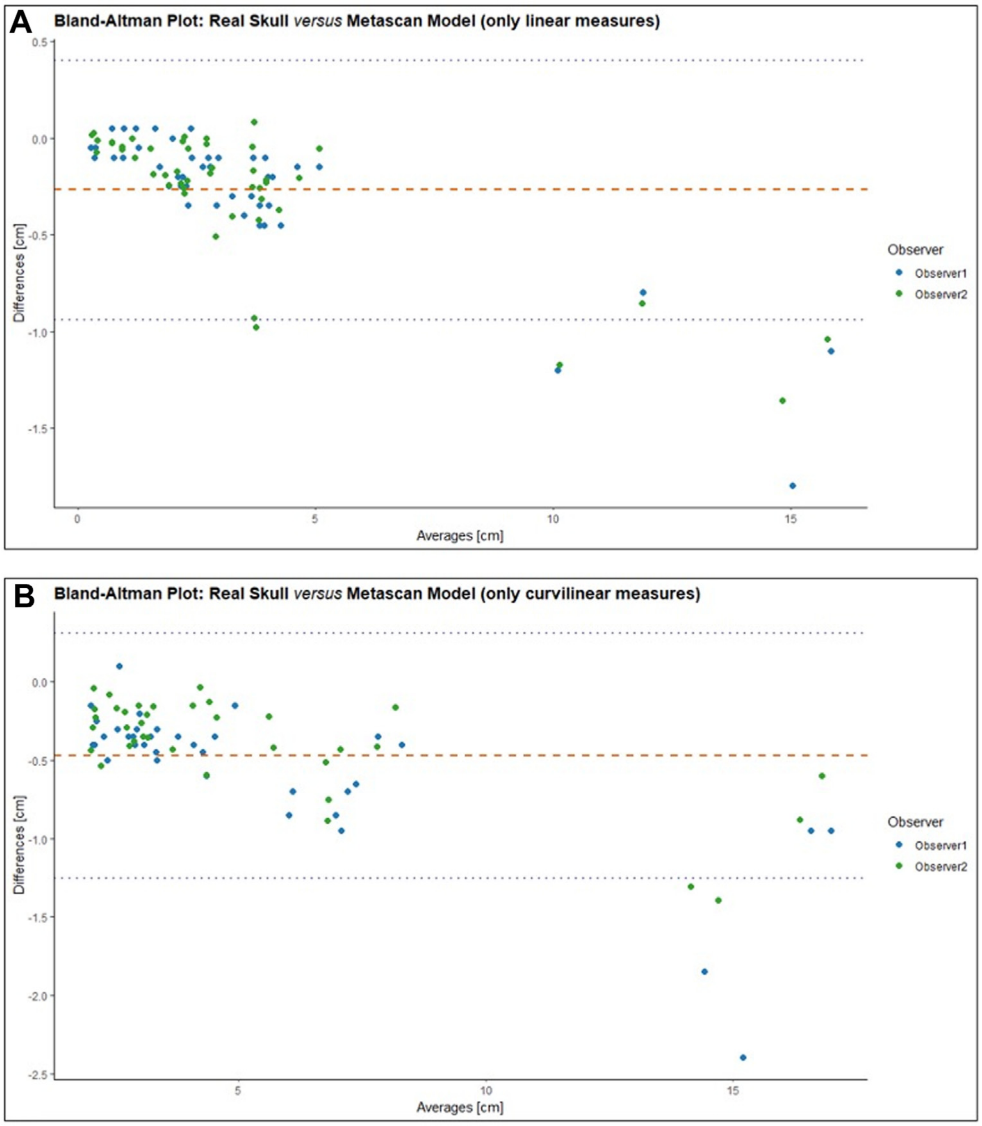

Supplementary Figure 1. Bland-Altman plots considering only linear measurements. (**A**) Agreement of linear measurements taken with Metascan model compared with direct measurements. A mean difference of −0.26 cm was found with lower limits of agreement (LoA) of −0.94 and upper LoA of 0.41. Notably, a systematic proportional bias was observed for measurements >5 cm. (**B**) Agreement of linear measurements taken with Agisoft Metashape model is shown compared with direct measurements. A mean difference of 0.04 cm was found with lower LoA of −0.12 and upper LoA of 0. 19.

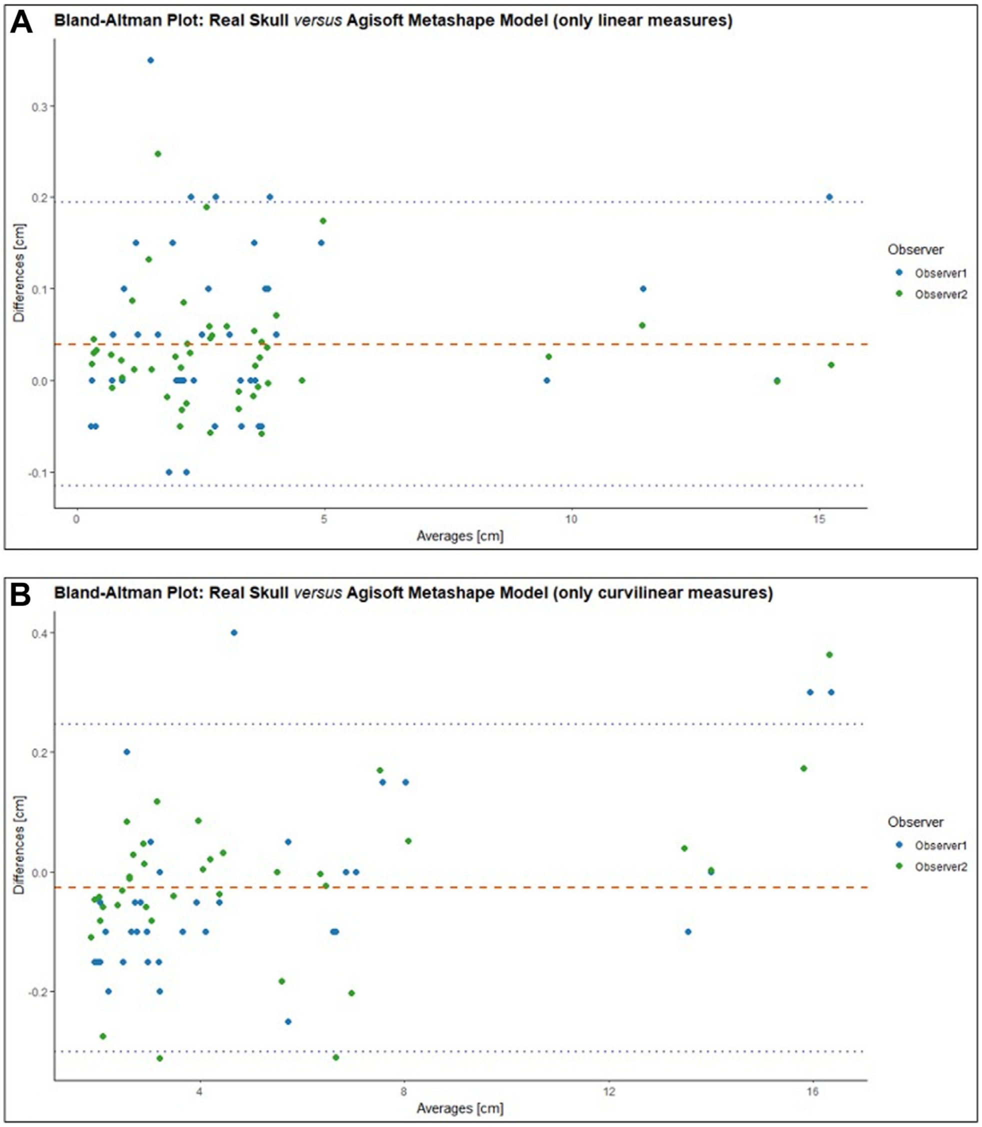

Supplementary Figure 2. Bland-Altman plots considering only curvilinear measurements. (**A**) Illustration of the agreement of curvilinear measurements taken with Metascan model compared with direct measurements. A mean difference of −0.47 cm was found with lower LoA of −1.26 and upper LoA of 0.31. Notably, a systematic proportional bias was observed for measurements >5 cm. (**B**) Agreement of curvilinear measurements taken with Agisoft Metashape model compared with direct measurements. A mean difference of −0.02 cm was found with lower LoA of −0.30 and upper LoA of 0.25.